ISSN 2249 –5460

Available online at www.internationaleJournals.com

INTERNATIONAL JOURNAL OF MATHEMATICAL SCIENCES, TECHNOLOGY AND HUMANITIES

International eJournals

International Journal of Mathematical Sciences, Technology and Humanities 124 (2014) 1331-1348

Effects Of Slip And Magnetic Field On Peristaltic Pumping Of A Couple Stress Fluids In An Inclined Asymmetric Channel

P.Vinod kumar[1] Y. V .K. Ravi Kumar [2] Shahnaz Bathul[3]

[1] Department of Mathematics, JNTU College of Engineering , Nachupally,Karimnagar, INDIA.
[2] Practice School Division, Birla Institute of Technology (BITS) – Pilani, Hyderabad, INDIA.
[3] Department of Mathematics, JNTU College of Engineering , Kukatpally, Hyderabad, INDIA.

Abstract: We have analyzed the on peristaltic pumping of a couple stress fluid in an inclined porous channel with the effects of slip and Magnetic field . Analytical expressions for the stream function, the axial pressure gradient, the axial velocity and the distribution of the current density across the channel are obtained using long wavelength approximation and low Reynolds number. The results for the axial veleciy,pressure gradient, pressure rise across the channel have been computed numerically and explained graphically. The results were studied for various values of the physical parameters of interest, such as the couple stress parameter(γ) , the Magnetic number (M), Froude number (Fr), slip Parameter(L),inclination α and the time averaged mean flow rate Q.

Keywords: Couple stress fluid , magnetic field ,porous channel.

INTRODUCTON:

The process of peristaltic transport is quite popular among the recent researchers in view of its several industry, engineering and physiological applications. Especially the peristaltic transport of non-Newtonian fluids is a topic of major interest of the researchers in the physiological world. In physiology, its occurrence in the transport of urine from kidney to bladder, chyme motion in the gastrointestinal tract, blood circulation in small blood vessels, movement of bile in the bile duct, ovum and sperm transport through respective reproductive ducts, etc. Blood pumps and heart lung machine also work under this process. In nuclear industry, a toxic liquid can be transported in order to avoid contamination of the outside environment by this process.
Latham [1] first initiated the concept of peristaltic mechanism. Later on, this mechanism has become an important topic of research owing to the above mentioned applications in biomechanical engineering and biomedical technology. Several investigators [2-5] have studied the peristaltic transport of fluids in tubes for better and clear understanding of peristaltic mechanism. Weinberg et al. [6] conducted an experimental study of peristaltic pumping, whereas Yin and Fung [7]] made a comparison between theoretical and experimental studies in peristaltic

transport. Misra and Pandey [8] gave a mathematical model for peristaltic transport of blood in small vessels. Further, Riaz et al. [9] studied the peristaltic transport of a Carreau fluid in a compliant rectangular duct by utilizing the assumptions of long wave length and low Reynolds number. Mekheimer et al. [10] put forwarded peristaltic motion of a particle–fluid suspension in a planar channel.

The study of a couple stress fluid plays key role in understanding various physical problems, because it possesses the mechanism to describe rheologically complex fluids such as liquid crystals, colloidal fluids, liquids containing long-chain molecules as polymeric suspensions, animal and human blood and lubrication.

Theory of couple stress fluid proposed by Stokes [11], defines the rotational field in terms of the velocity field for setting up the constitutive relationship between the stress and strain rate. Some theoretical studies [12–16] of blood flow indicate that some of the non-Newtonian flow roperties of blood may be explained by assuming the blood to be a fluid with couple stress. Valanis and Sun [17] and Pal et al. [18] studied on the couple stress fluid having applications in blood flow through cardiovascular system. Srivastava [19] have examined the peristaltic transport of a couple stress fluid under a zero Reynolds number and long wave length approximations. Rao and Rao [20] put forwarded the peristaltic flow of a couple stress fluid through a porous medium in a channel at low Reynolds number.

With the above discussion in mind, the goal of this investigation is to study the effect of slip and magnetic field on peristaltic pumping of a couple stress fluid model. The flow analysis is developed in a wave frame of reference moving with the velocity of the wave. In this paper the governing equations under the long wavelength and low Reynolds number approximation and the corresponding boundary conditions are prescribed and includes the analytical solution of the problem. The results for the axial velocity, stream function and pressure rise have been discussed for various values of the parameters in this problem. Also, the pumping characteristics, the contour plot for the magnetic force function and the trapping phenomena are discussed in detail in the same section. Finally, the main conclusions are summarized in.

2. Mathematical formulation:

Consider the flow of viscous ,an electrically and conducting incompressible couple-stress fluid flowing through an inclined porous channel of uniform thickness under the action of an external magnetic field. Let $\bar{\gamma} = h_1^{'}$ and $\bar{Y} = h_2^{'}$ represent respectively the upper wall and lower wall of the inclined channel. The medium is considered to be induced by a sinusoidal wave train propagating with a wave speed c along the length of the channel wall, such that

$$h_1^{'}(\bar{X},\bar{t}) = \bar{d}_1 + \bar{a}_1 \cos\left[\frac{2\pi}{\lambda}\left(\bar{X} - c\bar{t}\right)\right] \quad (1)$$

$$h_2^{'}(\bar{X},\bar{t}) = -\bar{d}_2 - \bar{b}_1 \cos\left[\frac{2\pi}{\lambda}\left(\bar{X} - c\bar{t}\right) + \phi\right] \quad (2)$$

where $\bar{d}_1$ and $\bar{d}_2$ are the mean height of the upper and lower wall of the channel from the central line, $\bar{a}_1$ and $\bar{b}_1$ are the amplitudes of waves of the channel walls, λ the wave length, ϕ ($0 \le \phi \le \pi$) the phase difference between the wave trains of both the walls, $\bar{X}$ and $\bar{Y}$ are the rectangular co-ordinates with $\bar{X}$ measures the axis of the channel and $\bar{Y}$ the traverse axis perpendicular to $\bar{X}$.

The fluid flow through the channel is exerted by an external transverse uniform constant magnetic field of strength B0, in which the induced magnetic field is neglected because of the low magnetic Reynolds number. Therefore the total magnetic field vector becomes $\vec{B}\ (0, B_0, 0)$.

The equations of motion for the flow through an inclined asymmetric channel obeying couple stress fluid with externally imposed magnetic field by neglecting the body couples are

$$\vec{\nabla} . \overrightarrow{V'} = 0 \tag{3}$$

$$\rho\left(\frac{\partial \overrightarrow{V'}}{\partial \bar{t}} + (\overrightarrow{V'} . \vec{\nabla})\, \overrightarrow{V'}\right) = -\nabla p' + \mu \vec{\nabla}^2 \overrightarrow{V'} - \eta \vec{\nabla}^4 \overrightarrow{V'} + \vec{J}\vec{B} + \rho g(\hat{i}\sin\alpha - \hat{j}\cos\alpha). \tag{4}$$

where $\overrightarrow{V'} = (U', V', 0)$ is the velocity vector, μ the viscosity of fluid, η the constant associated with couple stress, p' the fluid pressure, ρ the fluid density, σ the electrical conductivity, α the inclination of the channel, g be the acceleration due to gravity and $\vec{J}$ is the current vector due to Ohm's law, given by $\vec{J} = \sigma(\vec{E} + \vec{V}' \mathrm{X} \vec{B})$. The fourth term on the right hand side of Eq.(4) represent the body force per unit volume due to the application of an external magnetic field. Due to the assumption of low magnetic Reynolds number, the induced electric field is neglected. Therefore, the Ohm's law simply reduces to $\vec{J} = \sigma \vec{V}' \mathrm{X} \vec{B}$. It is noted that in our model there is no external electric field.

Analytical solution:

Let us consider a wave frame $(\bar{x}, \bar{y})$ that moves with the velocity c away from fixed frame $(\bar{X}, \bar{Y})$. Therefore we use the relation between wave frame and fixed frame of reference as follows

$$\bar{x} = \bar{X} - c\bar{t}\ ,\quad \bar{y} = \bar{Y}\ ,\quad \bar{u} = \bar{U} - c \text{ and } \bar{v} = \bar{V} \tag{5}$$

in which $(\vec{U}, \vec{V})$ and $(\vec{u}, \vec{v})$ are the velocity components in the fixed frame and wave frame of reference respectively. Due to the time dependence of the channel wall, in the laboratory frame $(\bar{X}, \bar{Y})$, the flow is unsteady. However, the coordinate frame moving with the wave speed c in the wave frame $(\bar{x}, \bar{y})$, the boundary shape becomes stationary and hence the flow in the wave frame is steady. Henceforward all the flow quantities analyzed in the wave frame of reference.

Let us introduce the following dimensionless variables

$$x=\frac{\bar{x}}{\lambda},\quad y=\frac{\bar{y}}{d_1},\quad h_1=\frac{\bar{h}_1}{\bar{d}_1},\quad h_2=\frac{\bar{h}_2}{\bar{d}_1},\quad u=\frac{\bar{u}}{c},\quad v=\frac{\lambda\bar{v}}{d_1 c},\quad p=\frac{\bar{d}_1^{\,2}}{c\lambda\eta}\bar{p},\quad t=\frac{c}{\lambda}\bar{t}.$$

(6)

Using the transformation (5) and the non-dimensional variables defined in Eq. (6) into the governing Eq. (4), the equations of motion in dimensionless form as well as in the wave frame can be written as

$$\begin{aligned}\mathrm{Re}\,\delta((u+1)\frac{\partial u}{\partial x}+v\frac{\partial u}{\partial y})&=-\frac{\partial p}{\partial x}+(\delta^2\frac{\partial^2 u}{\partial x^2}+\frac{\partial^2 u}{\partial y^2})-\frac{1}{\gamma^2}(\delta^4\frac{\partial^4 u}{\partial x^4}+\frac{\partial^4 u}{\partial y^4})-M^2(u+1)+\frac{\mathrm{Re}}{Fr}\sin\alpha,\\ \mathrm{Re}\,\delta^3((u+1)\frac{\partial v}{\partial x}+v\frac{\partial v}{\partial y})&=-\frac{\partial p}{\partial y}+\delta^2(\delta^2\frac{\partial^2 v}{\partial x^2}+\frac{\partial^2 v}{\partial y^2})-\frac{\delta^2}{\gamma^2}(\delta^4\frac{\partial^4 u}{\partial x^4}+\frac{\partial^4 u}{\partial y^4})-\frac{\mathrm{Re}\,\delta}{Fr}\cos\alpha.\end{aligned}\tag{7}$$

(8)

The dimensionless parameters that appear in Eqs. (7) and (8) can be defined as the Reynolds number $\mathrm{Re}=\frac{\rho c d_1}{\eta}$, Wave number $\delta=\frac{d_1}{\lambda}$, the couple stress number $\gamma=\frac{\eta}{\mu d_1^2}$ and the Froude number $\mathrm{Fr}=\frac{c^2}{qd_1}$.

Under the assumption of long wavelength (λ) that is $\delta\le 1$ and the low Reynolds number $\mathrm{Re}\le 1$ the Eqs. (7) and (8) simply reduce to,

$$\frac{\partial p}{\partial x}=\frac{\partial^2 u}{\partial y^2}-\frac{1}{\gamma^2}\frac{\partial^2 u}{\partial y^2}-M^2(u+1)+\frac{\mathrm{Re}}{Fr}\sin\alpha$$

(9)

$$\frac{\partial p}{\partial y}=0$$

(10)

$$\frac{1}{P_r}\frac{\partial^2\theta}{\partial y^2}+E_c\frac{\partial u}{\partial y}=0.\tag{11}$$

The volumetric flow rate in the fixed frame G' is given by

$$G'=\int_{\bar{h}_2}^{\bar{h}_{11}}\bar{U}(\bar{X}',\bar{Y}',\bar{t})d\bar{y}\tag{12}$$

where $\bar{h}_1$,and $\bar{h}_2$ are functions of $\bar{X}'$ and $\bar{t}$.

The rate of volume flow in the wave frame is "g "found to be given by,

$$g = \int_{\bar{h}_2}^{\bar{h}_{11}} \bar{u}(\bar{x}, \bar{y}) d\bar{y}$$

(13)

where $\bar{h}_1$,and $\bar{h}_2$ are functions of $\bar{x}$ alone.

Using the transformation $U' = u' + c$ from Eq.(5) in the Eq.(12) and using Eq.(13) the relation between G' and g can be written as

$$G' = g + c(\bar{h}_1 - \bar{h}_2) \tag{14}$$

The time mean flow rate over a period T at a fixed position $\bar{X}$ is defined to be

$$G = \frac{1}{T}\int_0^T G' dt.$$

(15)

Use of Eq. (14) in Eq. (15) the flow rate Q has the form

$$G = \frac{1}{T}\int_0^T G' dt + c(\bar{h}_1 - \bar{h}_2) = g + cd_1 + cd_2$$

(16)

The non-dimensional form of Eq. (16) yields

$$Q = F + 1 + d, \tag{17}$$

$$G = \frac{G'}{cd_1}, F = \frac{g}{cd_1} \text{ and } d = \frac{d_2}{d_1}.$$

(18)

Introducing the dimensionless stream function w by using $u = \frac{\partial \psi}{\partial y}$ and $v = -\delta \frac{\partial \psi}{\partial x}$ the expression for F has the form

$$F = \int_{\bar{h}_2}^{\bar{h}_{11}} \frac{\partial \psi}{\partial y} dy = \psi(h_1) - \psi(h_2).$$

(19)

By differentiating Eq. (9) partially with respect to y, we write the equation in terms of stream function ψ as

$$\frac{\partial^6 \psi}{\partial y^6} - \gamma^2 \frac{\partial^4 \psi}{\partial y^4} + \left(\gamma^2 M^2\right)\frac{\partial^2 \psi}{\partial y^2} = 0. \tag{20}$$

The boundary conditions for the present problem in terms of dimensionless stream function $\psi(x, y)$ in the wave frame can be written as

$$\psi = \frac{F}{2} \quad \text{at} \quad y = h_1$$

(21)

$\psi = -\frac{F}{2}$ at y= h_2

(22)

Slip boundary conditions:

$$\frac{\partial \psi}{\partial y} + L\frac{\partial^2 \psi}{\partial^2 y} = -1 \quad \text{at} \quad y= h_1$$

(23)

$$\frac{\partial \psi}{\partial y} - L\frac{\partial^2 \psi}{\partial^2 y} = -1 \quad \text{at} \quad y= h_2$$

(24)

Vanishing couple stress: $\frac{\partial^3 \psi}{\partial y^3} = 0$ at y= h_1 and y= h_2

(25)

$\theta = 0$ at y= h_1,

$\theta = 1$ at y= h_2.

(26)

Where $L = \frac{\sqrt{k}}{\alpha d_1} = \frac{\sqrt{Da}}{\alpha}$ the permeability parameter including slip, Da is the Darcy number , α is the slip parameter and k is the permeability.

The non-dimensional form of the equations of the channel walls in the wave frame of reference reduce to

$$h_1(x) = 1 + a\cos 2\pi x \quad \text{and} \quad h_2(x) = -d - b\cos(2\pi x + \phi)$$

(26)

Where $a = \frac{a_1}{d_1}, b = \frac{a_2}{d_1}, d = \frac{d_2}{d_1}$.

The sixth order differential Eq.(20) in w with constant coefficient has the general solution for ψ in the following form

$$\psi = A_1 + A_2 y + A_3 \cosh(m_1 y) + A_4 \sinh(m_1 y) + A_5 \cosh(m_2 y) + A_6 \sinh(m_2 y)$$

(27)

where m_1 and m_2 together with the expressions for six integrating constants A_1 , A_2 , A_3 , A_4 , A_5 , and A_6 are obtained by using boundary conditions given in the Eq. (21),(22),(23),(24), and (25) and we put them in the Appendix at the end of the conclusion section.

Once we determined those arbitrary constants, the expression for axial velocity u is obtained from the relation $u = \frac{\partial \psi}{\partial y}$ as

$$u = A_2 + m_1 A_3 \sinh(m_1 y) + m_1 A_4 \cosh(m_1 y) + m_2 A_5 \sinh(m_2 y) + m_2 A_6 \cosh(m_2 y)$$

(28)

Similarly, the expression for $\frac{dp}{dx}$ can be derived from Eq. (9) and hence the non-dimensional expression of pressure rise per wave length Δp can be obtained as,

$$\Delta p = \int_0^1 \frac{dp}{dx} dx.$$

(29)

Solve the equation (11) by using boundary conditions (26),then we get

$\theta = B_1 + B_2 y + \psi$

where ψ is given in Eqs. (27).

Numerical Results of analytical solution:

The analytical solution of the couple stress model is presented. The analytical expressions for the stream function, axial velocity,pressure gradient and pressure rise per wave length have been calculated numerically in this paper.

The effects of various parameters on axial velocity with y shown Fig (1)-(2) for different values of magnetic number M , slip parameter L . It is observed from Fig (1) that axial velocity decreases at the central line of the channel for the increase in magnetic number (M).The result from Fig (2) that axial velocity decreases at the central line of the channel for the increase in slip parameter (L).

Fig (3)-(7) display the pressure gradient for various values of Magnetic number M ,Couple stress parameter γ, Slip parameter L, Froude number Fr and slip parameter α. Fig (3) depicts the variation in axial pressure gradient for the variation in the Magnetic number M. It is observed that the pressure gradient increases when the Magnetic number M is increases. In Fig (4) depicts the variation in axial pressure gradient for the variation in the Couple stress parameter γ. It is observed that the pressure gradient increases when the Couple stress parameter γ is increases.

The variation in pressure gradient with different values of slip parameter L is shown in the Fig (5). We observe that the increasing values of slip parameter

L diminishes the pressure gradient. The variation in axial pressure gradient with different values of Froude number Fr, is an important result shown in Fig (6).We observe that the axial pressure gradient decreases as the Froude number increases. Fig (7) depicts the variation in pressure gradient with different slip parameter α. It is observed that the pressure gradient gradually decreases with the increases of slip parameter α.

The variation of pressure rise with Q is calculated from equation (9) for different values of the Couple stress parameter γ, Froude number Fr and slip parameter α and is shown in Fig.(8)-(10). In Fig.(8) it is clear that the pressure rise decreases with the increase of volumetric flow rate Q. whereas the pressure rise increases with the increase of the inclination angle α. However, from Fig.(9) we observe that the trend is reversed in the case of Froude number Fr. From Fig.(10) that the pressure rise decreases with the increasing values of couple stress parameter γ in the pumping region, while the pressure rise increases with the increase of γ.

The variations of temperature field θ with y are calculated from equation (11) for different values of the Magnetic number M ,Couple stress parameter γ, and Slip parameter L is shown in Fig.(11)-(13). It is observed that the temperature distribution decreases with an increase in M, γ and L.

TRAPPING PHENOMENA

Trapping is another interesting phenomenon of peristalsis in which streamlines under certain conditions split to trap a bolus. This trapped bolus pushed ahead along with the peristaltic wall with the likewise speed of wave. The effects of M and L on trapping can be seen through the Figs. (14) and (15). Fig.(14) displays that the volume of trapped bolus increases with an increase in the Magnetic number M. Streamlines patterns in Fig. (15) indicate that the volume of the trapped bolus decreases due to an increase in the values of the activation slip parameter L.

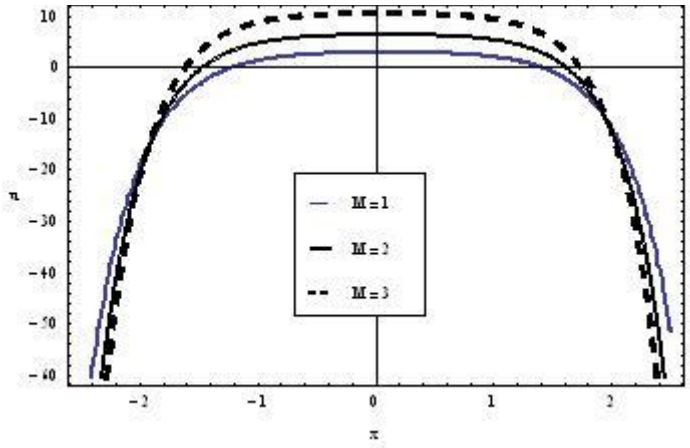

Fig. 1 Variation in axial velocity u for different values of M at x= 0 with positive flow rate Q=0.5 when L=1; γ=1.5; b=0.5; a=0.5; $\alpha = \pi/3$; d=1; $\phi = \pi/6$.

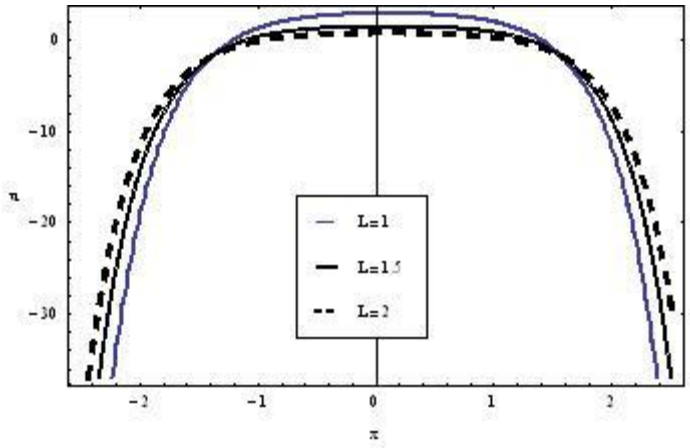

Fig. 2. Variation in axial velocity u for different values of L at x= 0 with positive flow rate Q=0.5 when L=1; γ=1.5; b=0.5; a=0.5; $\alpha = \pi/3$; d=1; $\phi = \pi/6$.

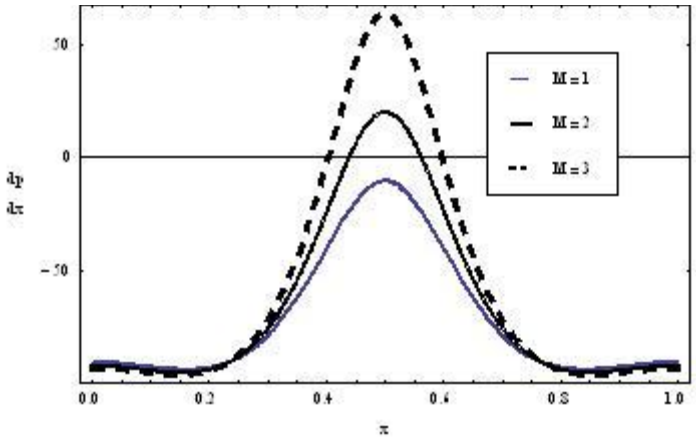

Fig. 3 Variation of pressure gradient dp/dx with x for different values of M at Fr=0.4 , L=1; γ =0.1; b=0.5; $\alpha = \pi/6$; a=0.5; d=1; ϕ=0.

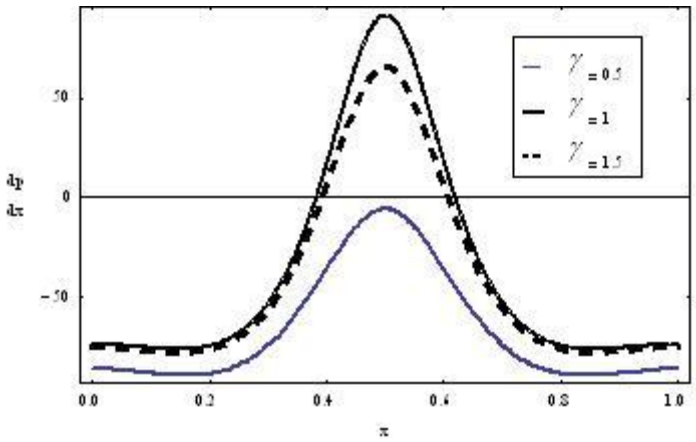

Fig. 4 Fig. 3 Variation of pressure gradient dp/dx with x for different values of γ at Fr=0.4 , L=1; γ=0.1; b=0.5; $\alpha = \pi/6$; a=0.5; d=1; ϕ=0.

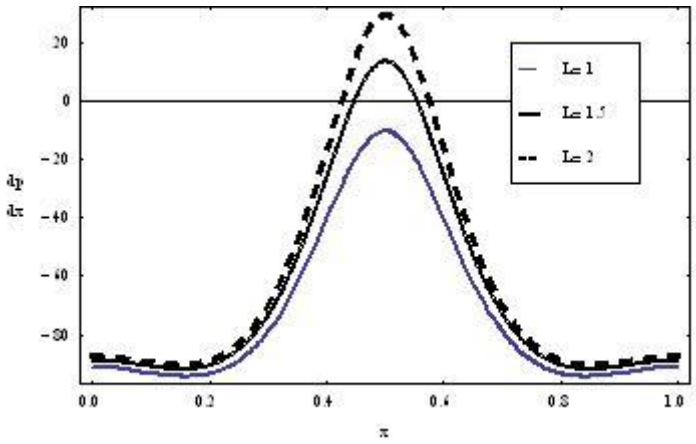

Fig. 5 Variation of pressure gradient dp/dx with x for different values of slip parameter L at Fr=0.4 , M=2; γ=0.1; $\alpha = \pi/6$;b=0.5;a=0.5;d=0.5; ϕ=0.

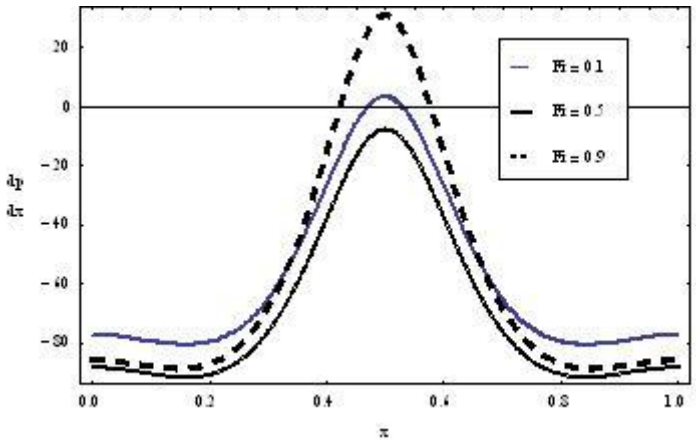

Fig. 6 Variation of pressure gradient dp/dx with x for different values of Froude number Fr at M=2; L=1; γ=5; $\alpha = \pi/6$;b=0.5;a=0.5;d=0.5; ϕ=0.

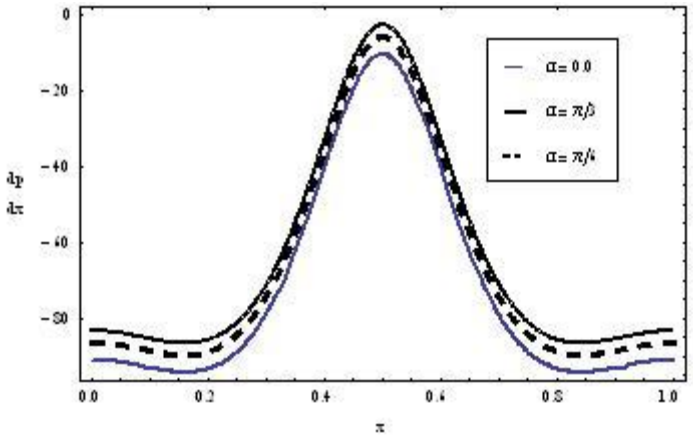

Fig. 7 Variation of pressure gradient dp/dx with x for different values Da at Fr=0.4 ; M=2; L=1; γ=0.1;b=0.5; $\alpha = \pi/6$; a=0.5;d=0.5; ϕ=0.

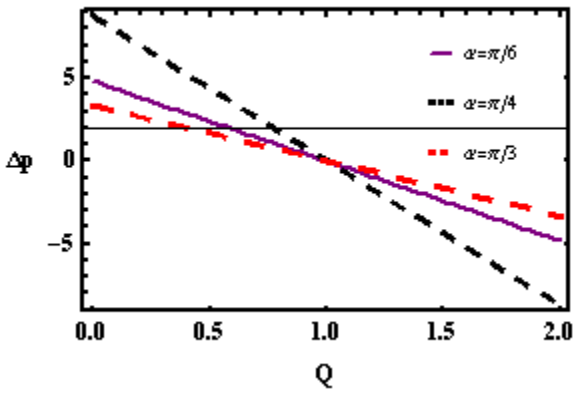

Fig. 8 Variation in pressure rises Δp with Q for different values of α , at Fr=0.4 ; M=2;L=1; γ =2.5; $\alpha = \pi/6$;b=0.5;a=0.5;d=1; ϕ =0.

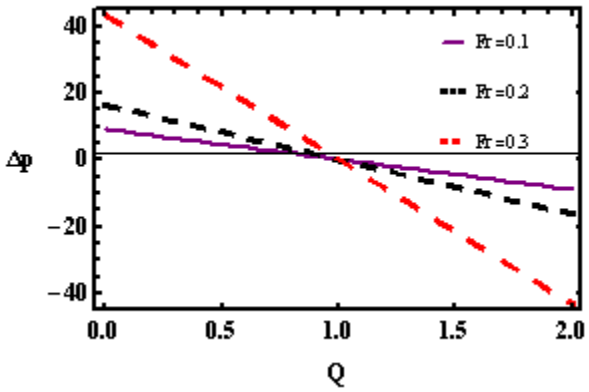

Fig. 9 Variation in pressure rises Δp with for different values of Froude number Fr at M=2;L=1; γ =2.5; $\alpha = \pi/6$;b=0.5;a=0.5;d=1; ϕ =0.

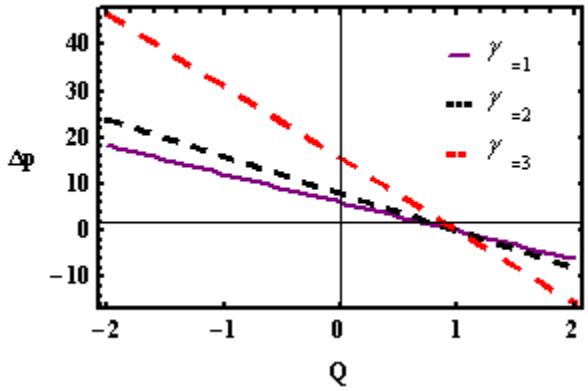

Fig. 10 Variation in pressure rise Δp for different values of slip parameter γ at Fr=0.4; M=2; L=1; $\alpha = \pi/6$;b=0.5;a=0.5;d=1; ϕ=0.

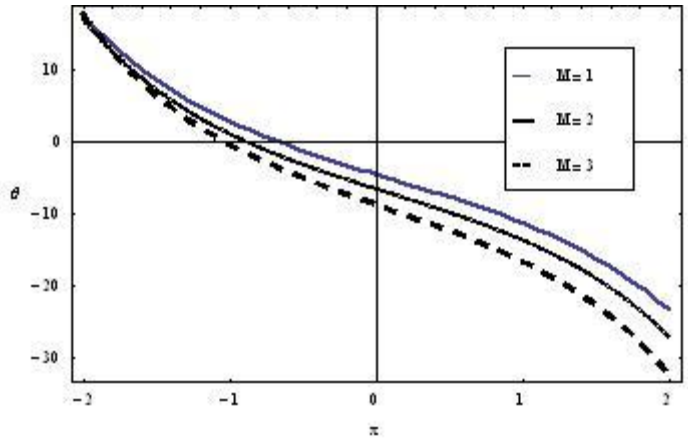

Fig. 11 Variation in θ for different values of slip parameter M at Fr=0.4; M=2; L=1; $\alpha = \pi$ /6;b=0.5;a=0.5;d=1; ϕ=0.

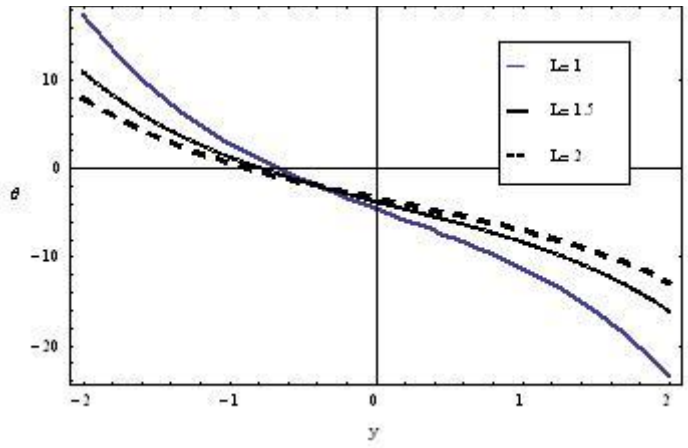

Fig. 12 Variation in θ for different values of slip parameter L at Fr=0.4; M=2; L=1; $\alpha = \pi$ /6;b=0.5;a=0.5;d=1; ϕ=0.

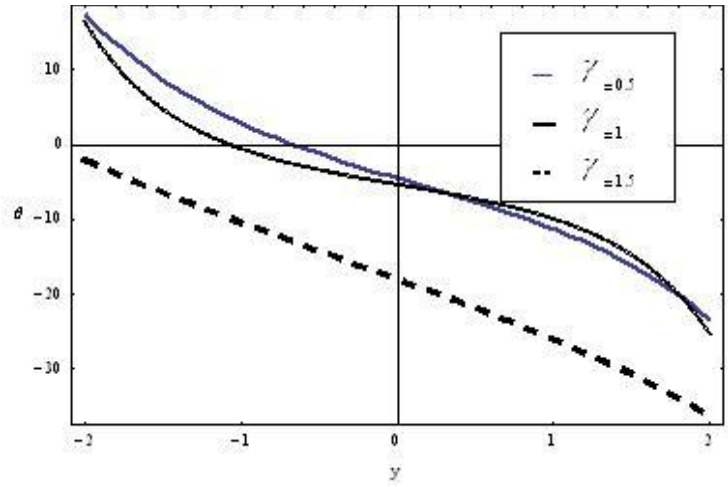

Fig. 13 Variation in θ for different values of slip parameter γ at Fr=0.4; M=2; L=1; $\alpha = \pi$ /6;b=0.5;a=0.5;d=1; ϕ=0.

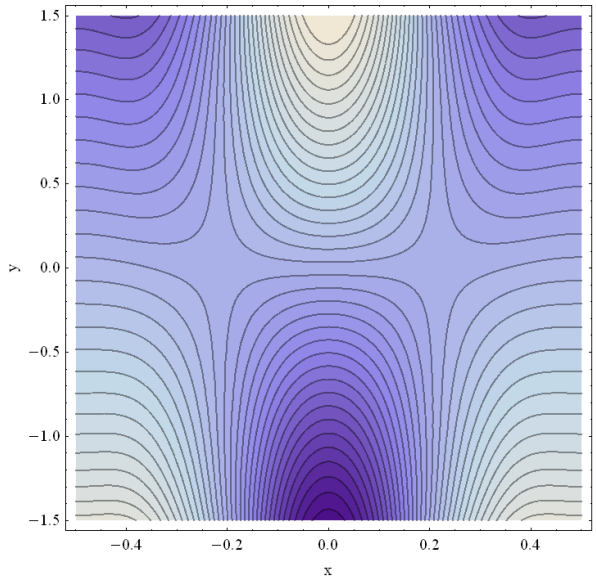

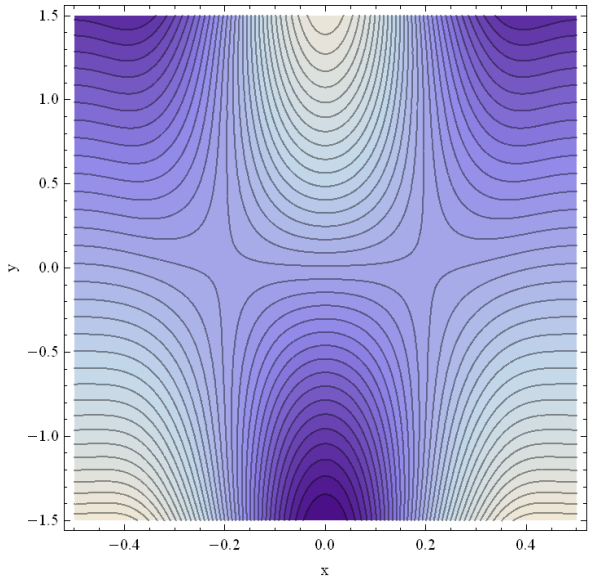

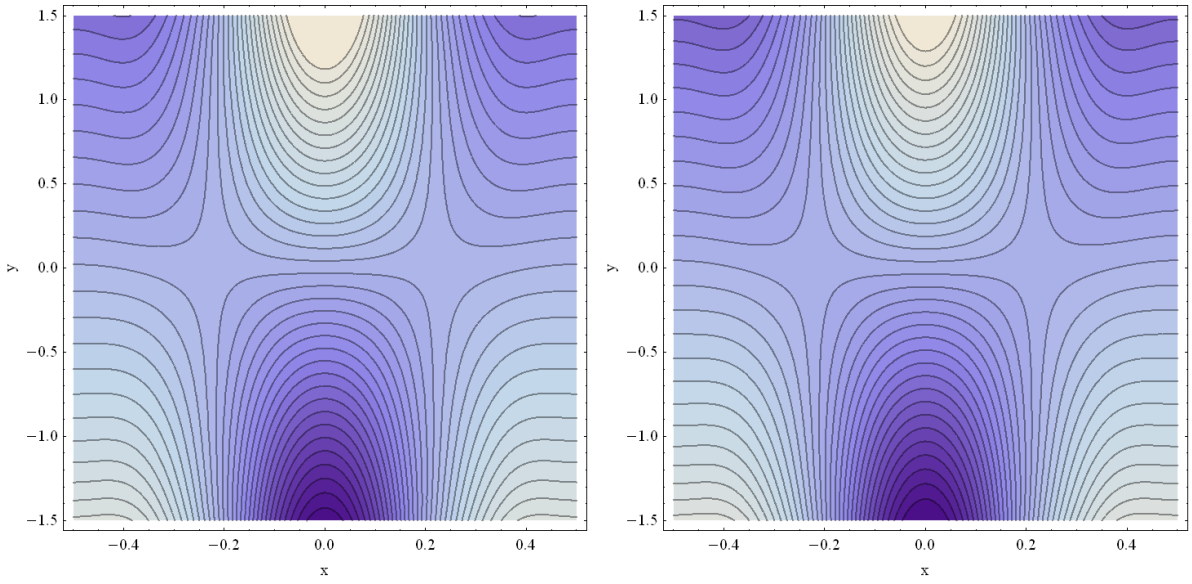

Fig 14 Distribution of stream lines in the presence of different strength of the magnetic field (M=2,2.5,3,3.5)with L =5; γ=1.5;b=0.4;a=0.5;d=1; ϕ=0.

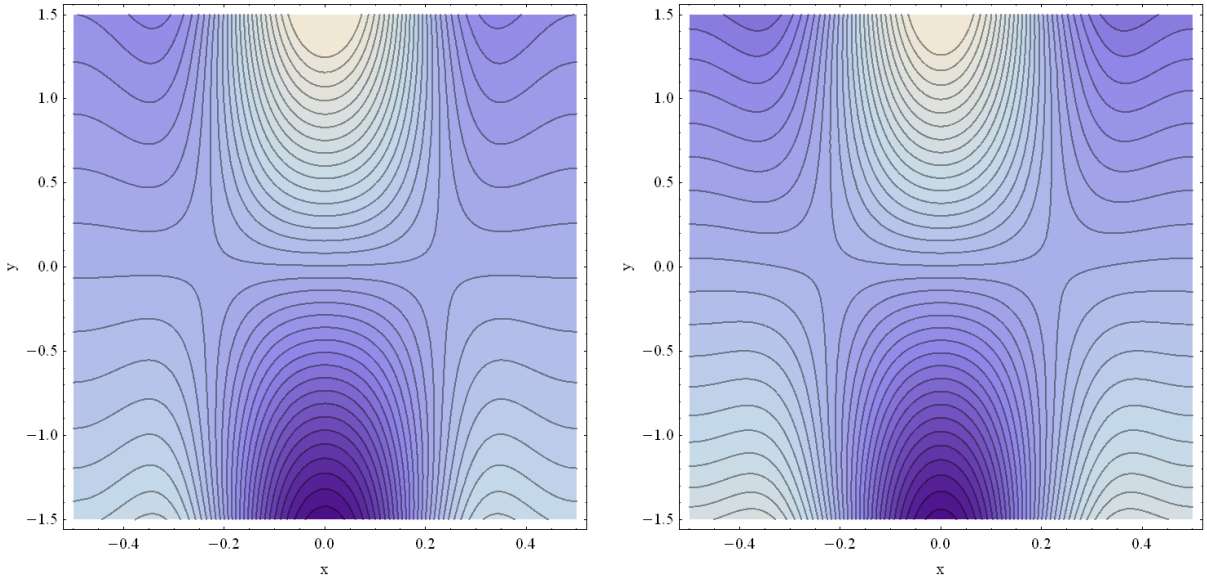

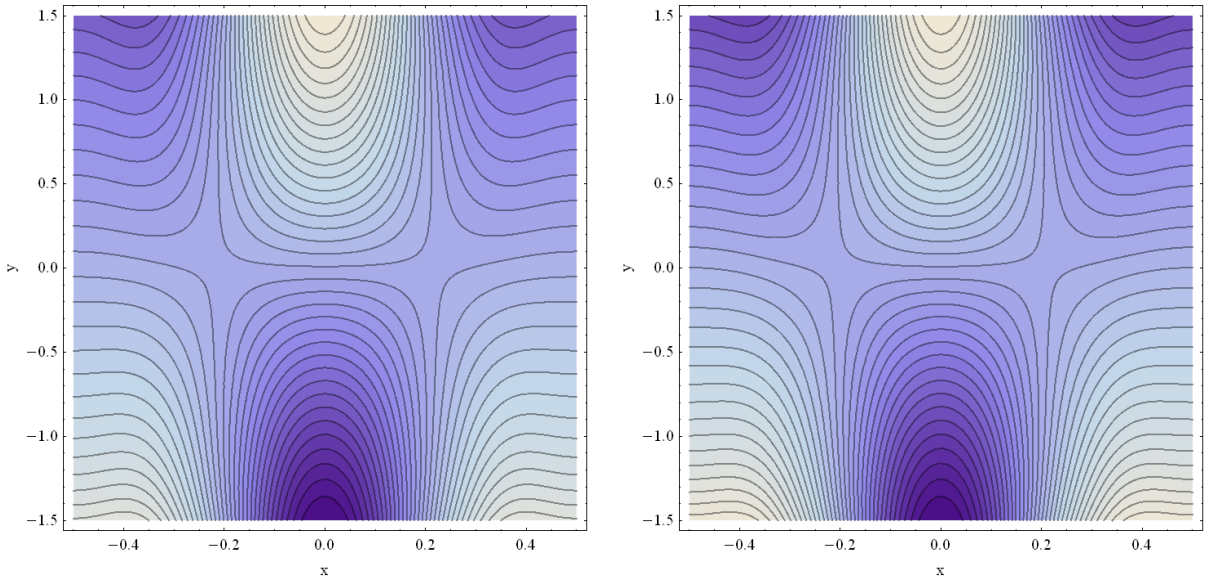

Fig 15 Distribution of stream lines in the presence of different values of slip parameter(L=1,1.5,2,2.5), M =2;Q=1.5; γ=5;b=0.4;a=0.5;d=1; ϕ=0.

Appendix A

The expressions that appear are listed as follows:

$$m_1 = \frac{1}{\sqrt{2}}\sqrt{(\gamma^2 + \sqrt{\gamma(\gamma^2 - 4M^2)})}$$

$$m_2 = \frac{1}{\sqrt{2}}\sqrt{(\gamma^2 - \sqrt{\gamma(\gamma^2 - 4M^2)})}$$

$$A_1 = \frac{1}{f_0}\left(A_3 f_{14} + A_4 f_{15} + A_5 f_{16} + A_6 f_{17} - f_9\right),$$

$$A_2 = -\left(1 + A_3 f_5 + A_4 f_6 + A_5 f_7 + A_6 f_8 - f_9\right),$$

$$A_3 = -\frac{(A_5 f_{31} + A_6 f_{32})}{f_{30}},$$

$$A_4 = -\frac{(A_5 f_{28} + A_6 f_{29})}{f_{27}},$$

$$A_5 = \frac{-(f_{26}(f_{36} - f_{34}))}{f_{35} f_{34} - f_{33} f_{36}},$$

$$A_6 = \frac{f_{26}(f_{35} - f_{33})}{f_{35} f_{34} - f_{33} f_{36}},$$

$$f_0 = h_1(x) - h_2(x)$$

$$f_1 = m_1 \sinh(m_1 h_1(x)) + Lm_1^2 \cosh(m_1 h_1(x)),$$

$$f_2 = m_1 \cosh(m_1 h_1(x)) + Lm_1^2 \sinh(m_1 h_1(x)),$$

$$f_3 = m_2 \sinh(m_2 h_1(x)) + Lm_2^2 \cosh(m_2 h_1(x)),$$

$$f_4 = m_2 \cosh(m_2 h_1(x)) + Lm_2^2 \sinh(m_1 h_1(x)),$$

$$f_5 = m_1 \sinh(m_1 h_2(x)) - Lm_1^2 \cosh(m_1 h_2(x)),$$

$$f_6 = m_1 \cosh(m_1 h_2(x)) - Lm_1^2 \sinh(m_1 h_2(x)),$$

$$f_7 = m_2 \sinh(m_2 h_2(x)) - Lm_2^2 \cosh(m_2 h_2(x)),$$

$$f_8 = m_2 \cosh(m_2 h_2(x)) - Lm_2^2 \sinh(m_1 h_2(x)),$$

$$f_9 = \frac{F(h_1(x) + h_2(x))}{2},$$

$$f_{10} = \cosh(m_1 h_1(x)) - \cosh(m_1 h_2(x)),$$

$$f_{11} = \sinh(m_1 h_1(x)) - \sinh(m_1 h_2(x)),$$

$$f_{12} = \cosh(m_2 h_1(x)) - \cosh(m_2 h_2(x)),$$

$$f_{13} = \sinh(m_2 h_1(x)) - \sinh(m_2 h_2(x)),$$

$$f_{14} = h_2(x)\cosh(m_1 h_1(x)) - h_1(x)\cosh(m_1 h_2(x)),$$

$$f_{15} = h_2(x)\sinh(m_1 h_1(x)) - h_1(x)\sinh(m_1 h_2(x)),$$

$$f_{16} = h_2(x)\cosh(m_2 h_1(x)) - h_1(x)\cosh(m_2 h_2(x)),$$

$$f_{17} = h_2(x)\sinh(m_2 h_1(x)) - h_1(x)\sinh(m_2 h_2(x)),$$

$$f_{18} = f_0 f_1 - f_{10,} \quad f_{19} = f_0 f_2 - f_{11,} \quad f_{20} = f_0 f_3 - f_{12,}$$

$$f_{21} = f_0 f_4 - f_{13,} \quad f_{22} = f_0 f_5 - f_{10,}$$

$$f_{23} = f_0 f_6 - f_{11,} \quad f_{24} = f_0 f_7 - f_{12,}$$

$$f_{25} = f_0 f_8 - f_{13,} \quad f_{26} = -(f_0 + F),$$

$$f_{27} = m_1^3(\sinh(m_1 h_2(x))\cosh(m_1 h_1(x)) - \sinh(m_1 h_1(x))\cosh(m_1 h_2(x))),$$

$$f_{28} = m_2^3(\sinh(m_1 h_2(x))\sinh(m_2 h_1(x)) - \sinh(m_1 h_1(x))\sinh(m_2 h_2(x))),$$

$$f_{29} = m_2^3(\sinh(m_1 h_2(x))\cosh(m_2 h_1(x)) - \sinh(m_1 h_1(x))\cosh(m_2 h_2(x))),$$

$$f_{30} = m_1^3(\sinh(m_1 h_1(x))\cosh(m_1 h_2(x)) - \sinh(m_1 h_2(x))\cosh(m_1 h_1(x))),$$

$$f_{31} = m_2^3(\sinh(m_2 h_1(x))\cosh(m_1 h_2(x)) - \sinh(m_2 h_2(x))\cosh(m_1 h_1(x))),$$
$$f_{32} = m_2^3(\cosh(m_1 h_2(x))\cosh(m_2 h_1(x)) - \cosh(m_1 h_1(x))\cosh(m_2 h_2(x)))$$

$$f_{33} = f_{20} - \frac{f_{18} f_{31}}{f_{30}} - \frac{f_{19} f_{28}}{f_{27}}, \qquad f_{34} = f_{21} - \frac{f_{18} f_{32}}{f_{30}} - \frac{f_{19} f_{29}}{f_{27}},$$
$$f_{35} = f_{24} - \frac{f_{22} f_{31}}{f_{30}} - \frac{f_{22} f_{28}}{f_{27}}, \qquad f_{36} = f_{25} - \frac{f_{22} f_{32}}{f_{30}} - \frac{f_{23} f_{29}}{f_{27}}.$$

$$B_1 = -(A_1 + A_2 h_1 + A_3\cosh(m_1 h_1) + A_4\sinh(m_1 h_1) + A_5\cosh(m_2 h_1) + A_6\sinh(m_2 h_1) + B_2 h_1;$$
$$B_2 = \frac{-(1 + D_1 - D_2)}{h_1 - h_2};$$
$$D_1 = A_1 + A_2 h_1 + A_3\cosh(m_1 h_1) + A_4\sinh(m_1 h_1) + A_5\cosh(m_2 h_1) + A_6\sinh(m_2 h_1);$$
$$D_2 = A_1 + A_2 h_2 + A_3\cosh(m_1 h_2) + A_4\sinh(m_1 h_2) + A_5\cosh(m_2 h_2) + A_6\sinh(m_2 h_2)$$

REFERENCES

[1] T.W. Latham, Fluid Motion in a Peristaltic Pumps, M.S. Thesis,MIT, Cambridge, MA, 1966.
[2] C.Barton,S.Raynor,Peristaltic flow in tubes,Bull. Bull. Math.Biophys. 30 (1968) 663–680.
[3] F.C.P. Yin, Y.C. Fung, Peristaltic waves in circular cylindricaltubes, J. Appl. Mech. 36 (1969) 579–587.
[4] T.S. Chow, Peristaltic transport in a circular cylindrical pipe,Trans ASME J. Appl. Mech. 37 (1970) 901–905.
[5] T. Colgan, R.M. Terrill, On peristaltic transport of fluids, J.Theoret. Appl. Mech. 6 (1) (1987) 3–22.
[6] S.L. Weinberg, E.C. Eckstein, A.H. Shapiro, An experimental study of peristaltic pumping, J. Fluid Mech. 49 (1971) 461–497.
[7] F.C.P. Yin, Y.C. Fung, Comparison of theory and experiment in peristaltic transport, J. Fluid Mech. 47 (1971) 93–112.
[8] J.C. Misra, S.K. Pandey, Peristaltic transport of blood in small vessels: Study of mathematical model, Comput. Math. Applic.43 (2002) 1183–1193.
[9] A. Riaz, R. Ellahi, S. Nadeem, Peristaltic transport of a Carreau fluid in a compliant rectangular duct, Alexand. Eng. J. 53 (2014)475–484.
[10] Kh. S. Mekheimer, E.E. El Shehawey, A.M. Elaw, Peristaltic motion of a particle–fluid suspension in a planar channel, Int. J.Theoret. Phys. 37 (1998) 2895–2920.

11] V.K. Stokes, Phys. Fluids 9 (1966) 1709.[12] K.C. Vanalis, C.T. Sun, Biorheology 6 (1969) 85.
[13] A.S. Popel, S.A. Regirer, P.I. Usick, Biorheology 11 (1974) 427.
[14] Kh.S. Mekheimer, Biorheology 39 (2002) 755.
[15] Kh.S. Mekheimer, Appl. Math. Comput. 153 (2004) 763.
[16] N. Ali, T. Hayat, M. Sajid, Biorheology 44 (2007) 125.

[17] K.C. Valanis, C.T. Sun, Poiseuille flow of a fluid with couple stress with applications to blood flow, Biorheology 6 (2) (1969)85–97.
[18] D. Pal, N. Rudraiah, R. Devanathan, A couple stress model of blood flow in the microcirculation, Bull. Math. Biol. 50 (4)(1988) 329–344.
[19] L.M. Srivastava, Peristaltic transport of a couple stress fluid,Rheol. Acta 25 (1986) 638–641.
[20] T.R. Rao, D.R.V.P. Rao, Peristaltic flow of a couple stress fluid through a porous medium in a channel at low reynolds number,Int. J. Appl. Math. Mech. 8 (3) (2012) 97–116.]